FULL PAPER

Deterministic quantum mechanics: The role of the Maxwell–Boltzmann distribution

Ralf C. Büchel | Dominik A. Rudolph | Irmgard Frank

Theoretische Chemie, Universität Hannover, Hannover, Germany

Correspondence
Irmgard Frank, Theoretische Chemie, Universität Hannover, Callinstr. 3A, 30167 Hannover, Germany.
Email: irmgard.frank@theochem.uni-hannover.de

Funding information
Gottfried Wilhelm Leibniz Universität Hannover; German Research Association

Abstract

To be accepted by the community, the claim that nuclear motion has to be treated classically must be tested for all kinds of phenomena. For the moment we claim that in a quantum chemical calculation, a classical description of nuclear motion is superior to the use of the Schrödinger equation, and investigate how far we get with this statement. In the present paper we address the question what nuclear quantum statistics means in this context. We will show that the Maxwell–Boltzmann velocity distribution evolves quickly in any molecular dynamics simulation and this guarantees the physically correct behavior of molecular systems. Using first-principles molecular dynamics simulations, or more precisely Car–Parrinello molecular dynamics, we investigate what this means for Bose-Einstein condensates and for Cooper pairs. It turns out that our approach can explain all relevant phenomena. As a consequence, we can introduce a deterministic formulation of quantum mechanics and can get rid of all the paradoxa in traditional quantum mechanics. The basic idea is to treat electrons and nuclei differently.

KEYWORDS

Bose–Einstein condensates, Car–Parrinello molecular dynamics, Cooper pairs, deterministic quantum mechanics, Maxwell–Boltzmann distribution

1 | INTRODUCTION

The ab initio simulation of the behavior of molecular systems during chemical reactions led us to claiming that nuclear motion is classical [1–3]. More precisely, the Schrödinger equation should not be applied to nuclear motion in a quantum chemical calculation. A classical treatment of nuclear motion greatly facilitates our view of quantum mechanics. We obtain a fully deterministic scheme. The central idea is to treat nuclear motion and electronic cloud with two different differential equations which are deterministic by nature. Only bound electrons should be described with the Schrödinger equation, because that is what the Schrödinger equation was made for. The quantum mechanical treatment of the electronic structure is essential and explains not only the hydrogen spectrum, but also molecular structure of any kind. Actually this includes the treatment of weakly bound electrons [4, 5], but not necessarily the treatment of the motion of completely unbound electrons, for which the fully relativistic Maxwell equations may be an alternative. At present, we have no single equation that would describe every phenomenon for any kind of particles at arbitrary temperatures. It is time to forget the idea that the Schrödinger equation could be that single equation. Nevertheless, the Schrödinger equation is extremely successful in describing bound electrons. We know today on the basis of millions of publications that the electronic structure of a molecular system as computed with the Schrödinger equation determines the arrangement of atoms and hence causes chemical bonding.

For arbitrary molecular structures this electronic many-body problem must be solved to describe lots of phenomena in the realm of chemistry or nanotechnology. The treatment of the many-particles wavefunction is greatly simplified by the introduction of orbitals, that is by decomposing the wavefunction into one-electron wavefunctions. The electrons are indistinguishable while the orbitals can be distinguished (1s, 2p, etc.), just like the nuclei (C_1, H_1, O_1, etc). In most quantum chemical calculations this electronic many-body problem is solved while the nuclei are just taken as point particles which are fixed in space.

To describe atomic or molecular motion and hence chemical reactions, Car and Parrinello developed Car-Parrinello molecular dynamics (CPMD) [6, 7]. "Molecular dynamics" normally means that the nuclei are described classically as moving point charges without further structure. In contrast to what is done in traditional molecular dynamics, Car and Parrinello chose to use a quantum mechanical treatment for the electrons. In the original and still widely used formulation of CPMD, the quantum mechanically computed electronic cloud moves quasi-classically and follows thus the motion of the nuclei. The alternative approach is Born–Oppenheimer molecular dynamics (BOMD) in which the electronic cloud is optimized self-consistently to the potential energy surface in every time step. Both approaches are summarized as first-principles molecular dynamics (FPMD) or ab initio molecular dynamics (AIMD). The electronic structure is normally computed using the density functional theory (DFT) approximation [8–10]. Both, CPMD and BOMD, are suited for simulating chemical reactions, with CPMD being less costly and more stable. Also it is appealing that the CPMD equations are derived from a single Lagrangian and that CPMD uses second derivatives with respect to time like the wave equation. Both with CPMD and BOMD, different reaction products can be formed in different simulation runs due to classical chaos.

In the present paper we compare properties as calculated using FPMD to experiment. First we have a look at the black body radiation, then we discuss Bose–Einstein condensates, and finally we investigate what all this means for the theoretical description of superconductivity. We are doing computations for molecular hydrogen as a light molecular system and sodium as a relatively light metal for which Bose–Einstein condensation has been reported. Finally we present computations on aluminum as it can be more easily converted into a superconductor than sodium.

For the moment we take it strictly for granted that nuclear motion is classical. We ask the question how far we get with this approach and where it clearly leads to deviations from experiment which cannot be explained by weaknesses of the density functional.

2 | METHOD

Car-Parrinello molecular dynamics simulations [6, 7] have been performed with the CPMD code [11] using the Becke–Lee–Yang–Parr (BLYP) functional [10, 12] in connection with the semi-empirical Grimme dispersion correction [13]. No dispersion correction was used for the sodium and aluminum calculations, because we found no systematic improvement. The spin-unrestricted version of Kohn–Sham theory was employed [14] whenever appropriate. Troullier–Martins pseudopotentials as optimized for the BLYP functional were employed for describing the core electrons [15, 16]. A non-linear core correction [17] was used for sodium and aluminum. The wavefunction cutoff which determines the size of the basis set was set to 50 Rydberg. The time step was chosen as 5 a.u. (0.12 fs) and the fictitious electron mass as 400 a.u. The simulations were run for 10 000–100 000 steps each, that is, for 1–12 ps.

For the simulations of hydrogen, the simulation cell was chosen as a cubic cell with the cell parameters $8.5 \times 8.5 \times 8.5$ Angstrom^3 ($16 \times 16 \times 16$ a.u.^{3}). For the simulations of sodium, we started from the crystalline structure. Our supercell for the bulk has the dimensions $17.1625 \times 17.1625 \times 17.1625$ Angstrom^3 ($32.4324 \times 32.4324 \times 32.4324$ a.u.^{3}) and contains 128 atoms. For the simulations of aluminum, the supercell of the crystal has the size $12.1017 \times 12.1017 \times 12.1017$ Angstrom^3 ($22.8689 \times 22.8689 \times 22.8689$ a.u.^{3}) containing 108 atoms. Clouds of atoms were formed by omitting some of the atoms from their places in the lattice or also manually using the Gaussview program.

Attempts to perform Born–Oppenheimer molecular dynamics simulations with the Gaussian code [18] for comparison were not successful: For performing a molecular dynamics run the self-consistent field convergence was way too bad, we could converge a few points only.

3 | RESULTS AND DISCUSSION

3.1 | The spectrum of a black body

There are three relevant formulas describing the spectrum of a black body [19]. First there is the Rayleigh–Jeans equation:

$$\phi(\lambda)d\lambda = \frac{2 \cdot c_0 \cdot \pi}{\lambda^4} k_B T \, d\lambda$$

As is well known, this relation leads to the ultraviolet catastrophe at high energies. It is often claimed that this is the classical limit for low energies. However, it was derived using the assumption that all oscillators have the same energy according to the equipartition of energy. This is not the correct classical limit. The equipartition theorem is certainly valid, however, it does not claim that there is the same amount of energy in every oscillator. It rather says that there is the same total energy in every degree of freedom. We observe a Maxwell–Boltzmann distribution of velocities as is shown in Figure 1.

FIGURE 1 Velocity distribution in Car–Parrinello molecular dynamics (CPMD) simulations. Black: A single hydrogen molecule: The classical limit is clearly visible. Red: If the molecule is allowed to interact with other molecules, it can also reach regions which are classically forbidden for a single oscillator. Green: If several molecules are monitored, the formation of a Maxwell–Boltzmann velocity distribution is observed. Blue: Maxwell–Boltzmann velocity distribution
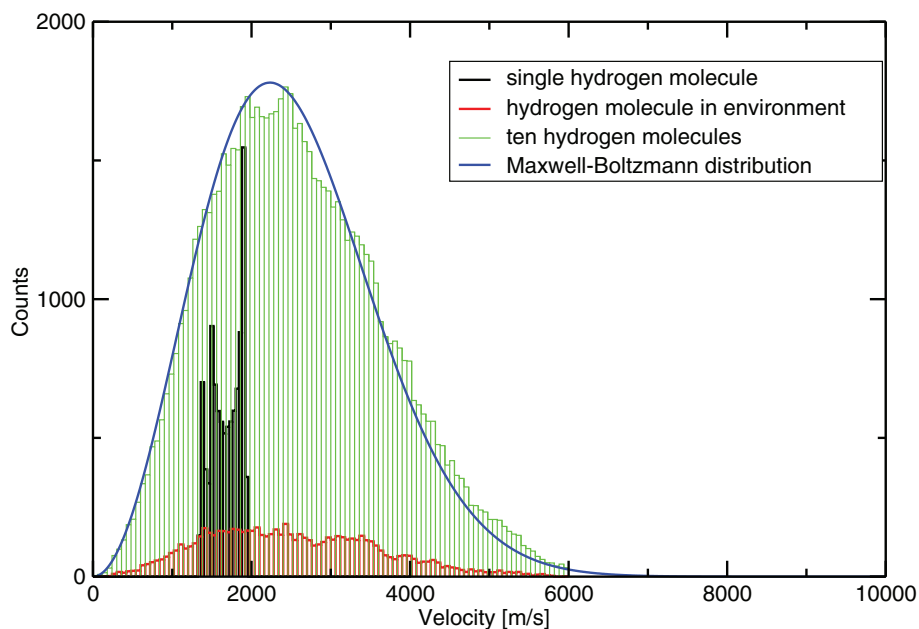
The general shape is similar to what was described by Wien:

$$\phi(\lambda)d\lambda = \frac{2 \cdot \pi \cdot h \cdot c_0^2}{\lambda^5} \cdot \frac{1}{e^{\frac{h \cdot c_0}{k_B \cdot \lambda T}}} \, d\lambda$$

This is not the original form of Wien's equation. It was the success of Planck to introduce the quantum of action, replacing the constants which Wien had introduced. Planck's law reads as follows:

$$\phi(\lambda)d\lambda = \frac{2 \cdot \pi \cdot h \cdot c_0^2}{\lambda^5} \cdot \frac{1}{e^{\frac{h \cdot c_0}{k_B \cdot \lambda T}} - 1} \, d\lambda$$

Numerically, the difference between the Wien and Planck distributions is small (see the Supporting Information).

The Maxwell–Boltzmann distribution of velocities reads as follows:

$$P(v)dv = 4\pi \left(\frac{m}{2\pi k_B T} \right)^{3/2} v^2 \frac{1}{e^{\frac{mv^2}{2k_B T}}} \, dv$$

It develops quickly in a simulation because it is the most likely distribution. The basis for this observation is Newton dynamics, that is, the idea that every object moves with constant velocity unless a force is acting. If there is a force, the acceleration is computed according to Newton's second law, $F = m\,a$. It is not so easy to find a similar theoretical framework which would lead to Planck's law instead of Wien's law. Since the numerical difference between Planck's law and Wien's law is small, it is not easy to come to a final conclusion what models the experimental black-body radiation or the AIMD simulation result more closely (see Figure 1 and the Supporting Information). To be able to compare to the normal way the black-body radiation is plotted, it is just necessary to plot the Maxwell–Boltzmann distribution weighted with v^2 versus $1/v^2$ (Figure 2).

To conclude, the simple picture that every atom moves linearly as long as no force is acting, allows to model complex phenomena like the Maxwell–Boltzmann distribution and the black-body radiation most straight-forwardly in FPMD simulations. While programming what leads to Wien's law seems most straight-forward, it is not clear how one could modify such simulations in a simple and convincing way to make them obey Planck's law. Experiment does not help much as the difference is small. Also relativistic effects are unlikely to cause the difference as the difference is largest for high wavelengths. It cannot be excluded at the moment that the specific interaction between radiation and matter leads to Planck's law, instead of Wien's law, on the basis of a Maxwell-Boltzmann distribution. Even if this were true, no change to molecular dynamics codes is necessary to describe nuclear motion. In any case we can safely forget the Rayleigh-Jeans formula as classical limit.

4 | BOSE–EINSTEIN CONDENSATES

The Bose–Einstein condensation is often taken as a proof that very small and very cool systems behave quantum mechanically. It has been first observed for ruthenium [20, 21] which is intriguing. Following the standard picture of quantum effects, one would rather have expected it to occur for the light,
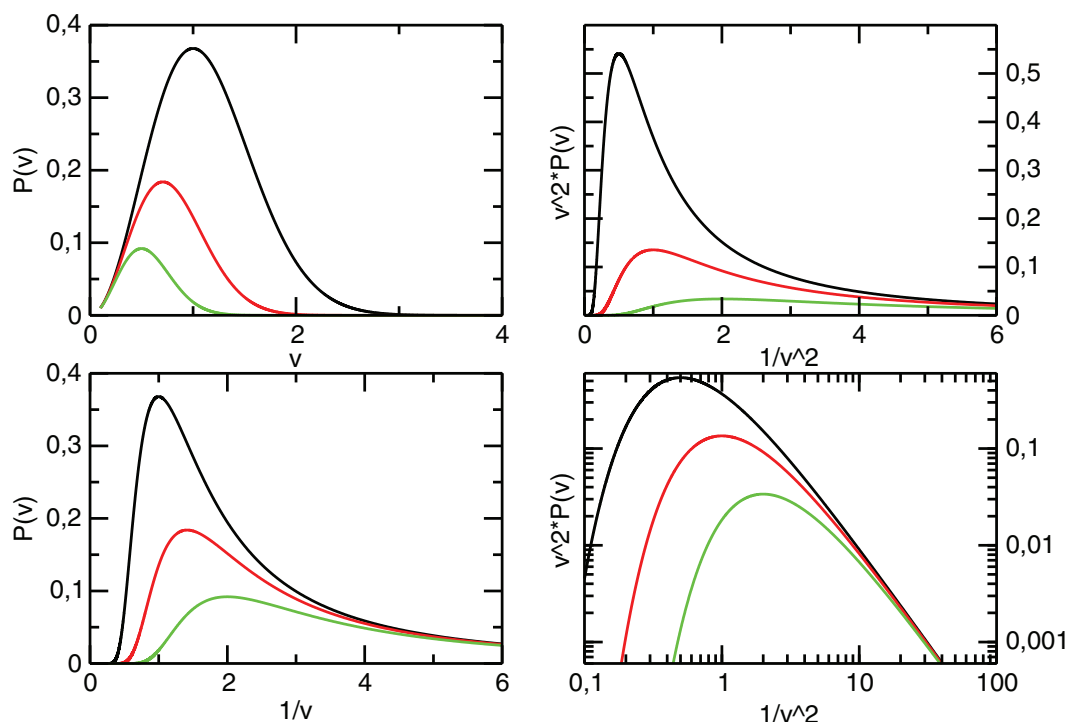
FIGURE 2   Different ways of plotting the Maxwell–Boltzmann distribution. If it is plotted against $1/v^2$ which is proportional to the wavelength, it resembles the black-body radiation curve. This is also true for a logarithmic representation which is often used when plotting the solar spectrum
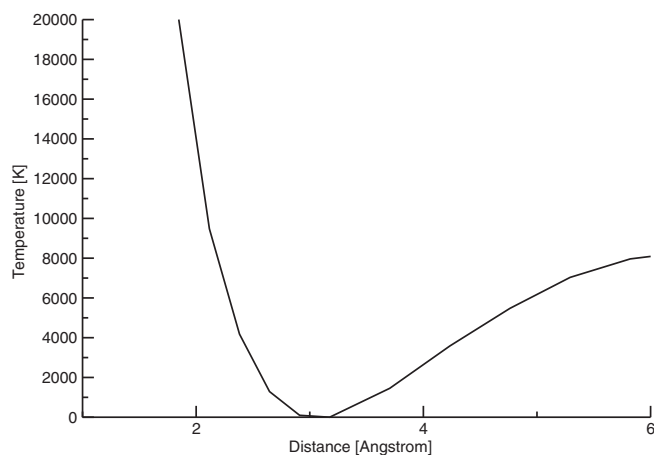

FIGURE 3   Potential for the Na—Na distance as computed using density functional theory showing how much kinetic energy is set free when the particles move with respect to another. As is typical for covalent bonds, a Morse potential is obtained. Given is the temperature in Kelvin as computed using the formula $E = kT$

bosonic helium atom. For ruthenium there is one more problem, namely the strongly attractive potential between ruthenium atoms. In a molecular cloud, the atoms always move relative to each other. Typical chemical energies of about 1 eV correspond to roughly 10 000 K (Figure 3).

That means that motion on a Morse potential, or, more generally, on a potential energy landscape causes high temperature changes. If we allow a system consisting of sodium atoms [22] to move in a FPMD simulation, it heats up quickly (Figures 4 and 5).

Only if we set up a perfectly crystalline structure of sodium atoms, the temperature stays close to zero. If we start from a cloud with distances larger than in the crystal, we observe the formation of clusters. Hence, from the results of molecular dynamics simulations, the condensation is a normal condensation to a strongly disordered solid (Figure 6). There is nothing which could possibly prevent condensation to a normal solid.

How is it possible to observe so low temperatures in this steep potential-energy hypersurface landscape? The answer is the way the temperature is measured: After the experiment the trap is turned off and the condensate may collide with a screen or its shadow may be detected on a screen. From the size of this spot the vertical velocity can be computed. For a classical condensate, a very small spot and hence a small "temperature" is measured. The true temperature as derived from the velocities within the condensate may be much higher. If there were such a thing as a Bose–Einstein condensation that is different from a normal condensation, it is not clear what prevents normal solids from a Bose–Einstein condensation, when cooled down. Invoking Feshbach resonances does not help as we are in a regime where the excited state is not markedly

FIGURE 4 Snapshots of the condensation of a sodium cloud to clusters. The cloud was formed by omitting atoms from a sodium crystal. (See the Supporting Information for different starting conditions.) the ionic temperature was set to zero. Initially the atoms approach the center of the system and gain energy quite quickly. During the first picosecond of the simulation, the system reaches temperatures of 600–700 K. this causes a reverse motion, the atoms do not immediately stick together. It takes some more picoseconds till two small clusters are formed
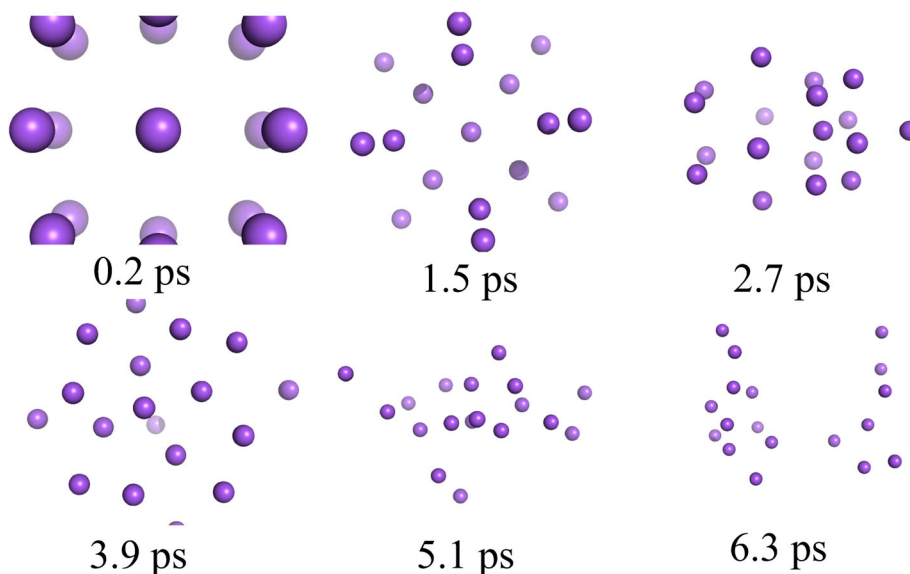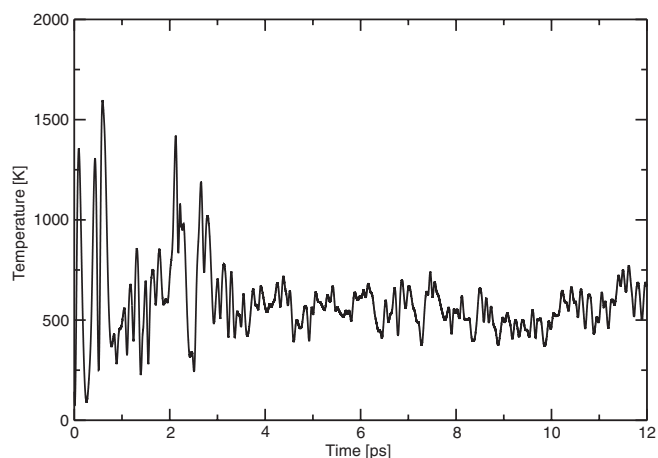

FIGURE 5 Temperature change during the molecular dynamics simulation run described in Figure 4

populated. Return to the ground state is quick from such a resonance, hence it has a zero net effect. It does not add energy to the total system nor remove it.

In addition, it does not change the atomic distance much. Also the claim that at low densities the normal condensation is too slow represents no satisfying explanation. Once there is a condensation nucleus, further condensation is rapid, as our simulations illustrate. Collisions must be allowed to achieve evaporative cooling and at extremely low temperatures these collisions are in part inelastic.

How can we find out if normal condensates or Bose–Einstein condensates are obtained? An experimental check could be to cool the system to 0.0001 K instead of 0.000001 K. This should generate a much smaller Bose–Einstein condensate: the higher the temperature, the shorter is the wavelength if one assumes a correlation of the de-Broglie formula with a temperature. Today it is possible to monitor way smaller objects than the initially reported Bose–Einstein condensates. On the nanometer scale it should be possible to find Bose–Einstein condensates already for temperatures of about 0.0001 K. On the contrary, the size of a normal condensate should not change much when going from 0.0001 to 0.000001 K or vice versa as long as the number of particles stays constant.

Another check could be to perform the experiment for a classical cluster for comparison. In experiment, the temperature is calculated from the extension of the spot measured. The low extension observed might just as well be due to the observation of very small classical clusters instead of a very cool cloud.

5 | SUPRACONDUCTIVITY

What about Cooper pairs [23, 24]? Shouldn't we observe them at such low temperatures?

Metals are normally described by band structure calculations performed at zero Kelvin. While also using DFT, we use a slightly different approach. Instead of computing the electronic wavefunction for the unit cell only and to obtain the rest by symmetry considerations, we use a

super cell consisting of many unit cells. This is the only meaningful approach if we want to do Car–Parrinello molecular dynamics, because we want as many atoms as possible moving independently. To analyze the electronic structure we compute maximally localized Wannier orbitals [25–27], that is, localized orbitals, and we determine their centers. Wannier functions as implemented in CPMD are obtained from the variational Kohn–Sham orbitals by minimizing the spread in an unitary transformation. Their counterparts for non-periodic systems are the Foster–Boys orbitals [28]. Like the wavefunction, Wannier orbitals and their centers are mathematical constructs without physical meaning. Nevertheless, orbitals are helpful when describing phenomena at the sub-nanometer scale. This is evident since the work of Woodward and Hoffmann who explained chemical reactivity on the basis of orbital symmetry [29]. The densities of the occupied orbitals add up to the total density, which gives
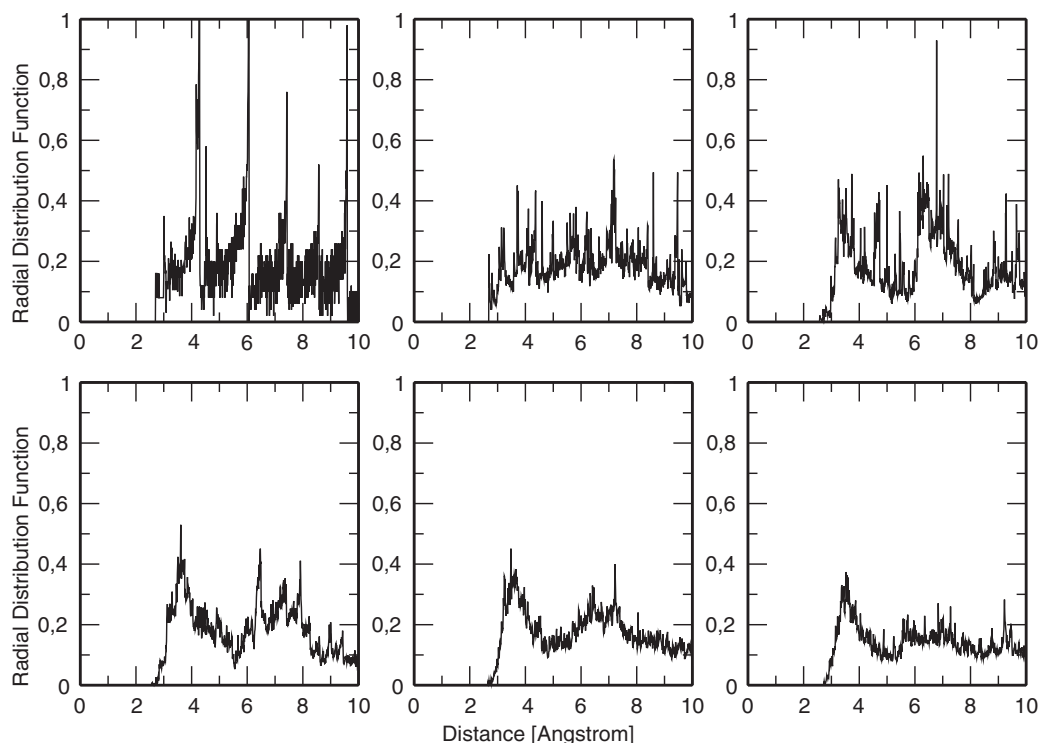

FIGURE 6   Radial distribution functions showing the Na—Na distances during different phases of the condensation, compare Figure 4. A disordered solid is formed very quickly
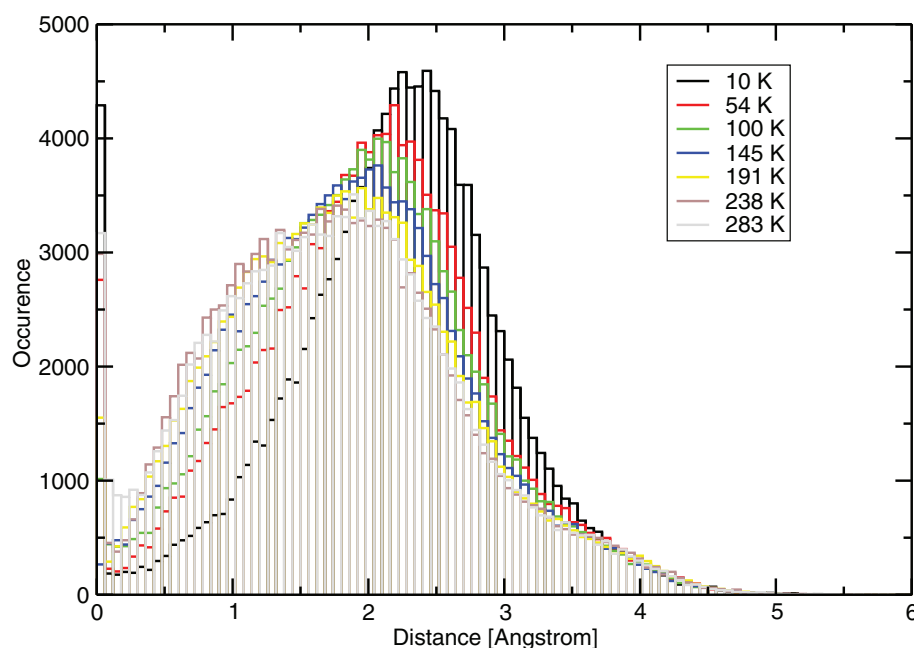

FIGURE 7   Relative distance of the Wannier centers ("electrons") in a sodium crystal, accumulated during a molecular dynamics run. In the beginning, the wavefunction is optimized to zero Kelvin. This is connected with the formation of electron pairs of all valence electrons (zero distance). The higher the temperature in the molecular dynamics run, the sooner the electron pairs split and avoid each other

their analysis a certain justification. The Wannier centers behave very much like electrons in a classical picture, however, one has to keep in mind that a cloud of water vapor is not identical to an accumulation of single rain drops. We monitor the relative distances of these Wannier centers.

At very low temperatures (<1 K) we only observe pairs of electrons, that is, the Wannier orbitals are centered at the same point in space and have the same spread. At higher temperatures, the electron pairs split (Figures 7 and 8). Here we observe something that is in part similar to Cooper pairs (Figure 9, see also the Supporting Information). An apparent difference is that our pairs are quantitatively everywhere, they are the normal ground state at temperatures close to zero Kelvin. With increasing temperature they are destroyed. Hence, the question to ask is not, how
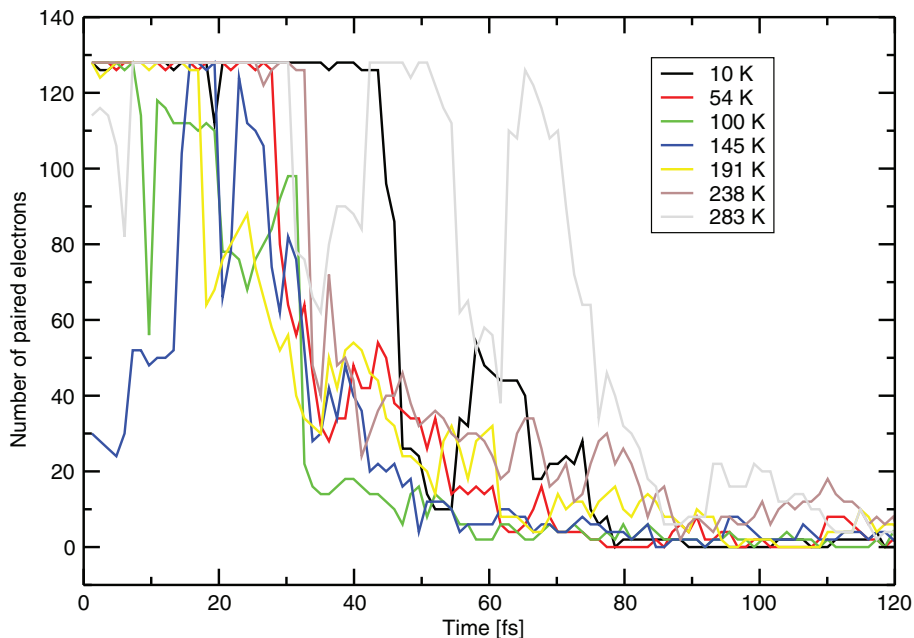

FIGURE 8 Number of paired electrons in the supercell, compare Figure 7. With raising temperature, the pairs live shorter. The gray line at the highest temperature is an exception, here the system oscillates forth and back between the two states
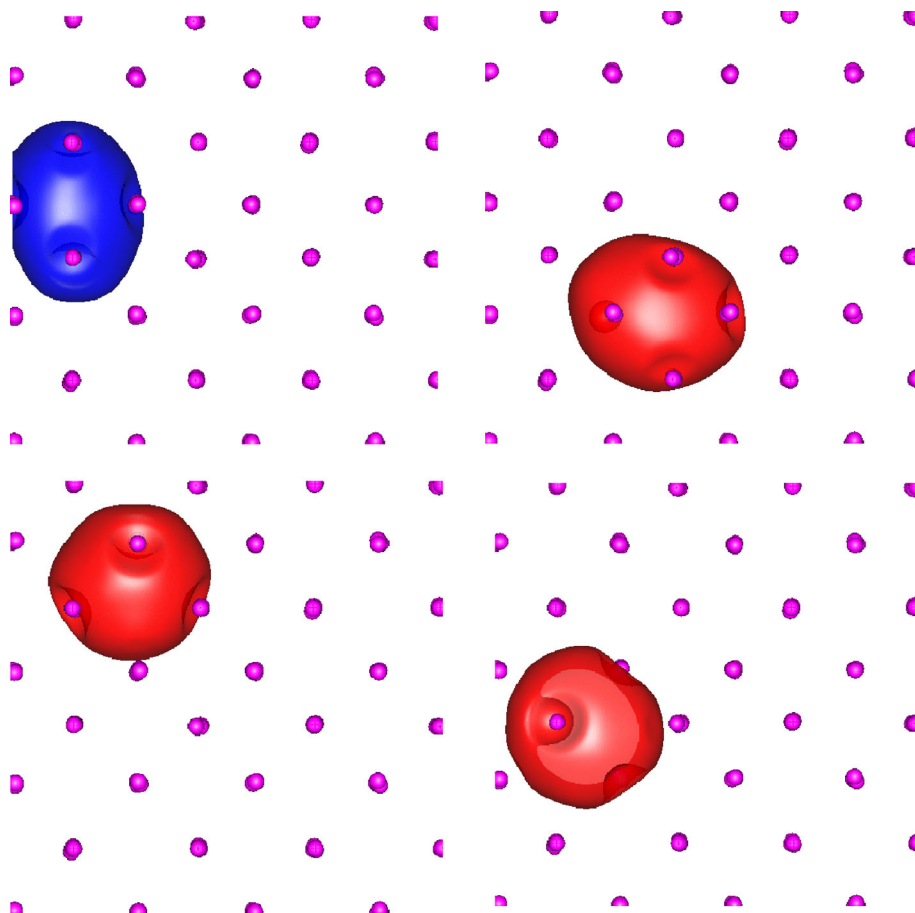

FIGURE 9 Shape of single paired Wannier orbitals in a sodium crystal. Their centers are located at interstitial positions within the crystal. The total valence density is obtained by summing up the densities of all the orbitals in the unit cell (128 orbitals in this case)

supraconductivity can form at low temperatures. The question to ask is, how electrical resistance is formed at higher temperatures. In other words, our simulations lead to the idea that it is not the electron–phonon coupling which causes Cooper pairs, it is rather the absence of phonons near zero Kelvin. The electron pairs in a metal are essentially free at low temperatures and, naively, one might expect that higher energies favor a fast motion. As we all know, the opposite is the case: metallic conductance decreases with rising temperature. In the present picture this is explained by the breaking of electron pairs leading to traps for the electrons. Note that the orbital picture represents an approximation in every practical calculation and that the decomposition into localized Wannier orbitals is arbitrary and may depend on the computer code employed.

It is not known if the DFT level is sufficient for the description of superconductivity. Hence it must be emphasized that we do not know if our observation is really connected to Cooper pairs. Nevertheless we can state that we observe a characteristic change at low temperatures which could be an explanation for superconductivity. How could this be checked experimentally? A possibility is to verify that electrons move in pairs instead of moving as single electrons at ultracold conditions.

6 | CONCLUSIONS

By using different differential equations for nuclear motion and the motion of the electronic cloud, as suggested by Car and Parrinello, we obtain a convincing picture of several condensed phase properties. A Maxwell–Boltzmann distribution is formed quickly already for small systems and short simulation times. Apparently, this distribution can be taken as the basis for computing the black-body radiation. Even if the picture is classical, we observe no UV catastrophe. We continue by applying our classical description to the Bose–Einstein condensation and doubt the usual interpretation of the experiments. A classical condensate explains all the experimental observations. Finally we investigate maximally localized Wannier functions and find that they have much in common with Cooper pairs, but that they describe the normal ground state at low temperatures in the absence of phonons. An ultimate proof that pairs of Wannier functions could be identified with Cooper pairs is certainly missing, however, we obtain a reasonable model of the behavior of metals at very low temperatures.

Our calculations are perfectly deterministic. If we do the same calculation two times, we get exactly the same result. If we make but small changes, we can get completely different reaction products. What does that mean for the philosophy of quantum mechanics? First, both Demokrit and Heraklit were right: We have atoms and we have an electronic wavefunction describing any kind of matter, thus "everything flows." We have a purely deterministic picture, hence Einstein was right: God does not play dice. Actually it is also true that every dice in this world is thrown by God. Schrödingers cat and the Einstein-Podolsky-Rosen (EPR) paradoxon represent no problems in a purely deterministic world, nor does the measurement problem in general. Every part of the system moves deterministically according to the respective equation of motion. This beautiful picture was obtained by treating only the electronic cloud quantum mechanically. A more complete picture would treat the inner structure of the nuclei, allowing for fission and fusion at high temperature and pressure. There is, however, no reason to use the Schrödinger equation for describing the inner structure of the nuclei.

AUTHOR CONTRIBUTIONS

Ralf Büchel: Investigation; validation; visualization; writing-review and editing. **Dominik Rudolph:** Investigation; validation; visualization; writing-review and editing. **Irmgard Frank:** Conceptualization; investigation; methodology; project administration; supervision; writing-original draft.

ORCID

Irmgard Frank https://orcid.org/0000-0001-9871-5183

REFERENCES

[1] I. Frank, arXiv, 1402.1133 **2014**.
[2] I. Frank, arXiv, 1605.06954 **2016**.
[3] I. Frank, S. Genuit, F. Matz, H. Oschinski, *Int. J. Quantum Chem.* **2020**, *120*, e26142.
[4] M. Boero, *J. Phys. Chem. A* **2007**, *111*, 12248.
[5] M. Pizzochero, F. Ambrosio, A. Pasquarello, *Chem. Sci.* **2019**, *10*, 7442.
[6] R. Car, M. Parrinello, *Phys. Rev. Lett.* **1985**, *55*, 2471.
[7] D. Marx, J. Hutter, *Ab Initio Molecular Dynamics: Basic Theory and Advanced Methods*, Cambridge University Press, Cambridge **2009**.
[8] P. Hohenberg, W. Kohn, *Phys. Rev. B* **1964**, *136*, 864.
[9] W. Kohn, L. J. Sham, *Phys. Rev. A* **1965**, *140*, 1133.
[10] A. Becke, *Phys. Rev. A* **1988**, *38*, 3098.

[11] CPMD. Version 4.1, J. Hutter et al. http://www.cpmd.org/, Copyright IBM Corp 1990–2015, Copyright MPI für Festkörperforschung Stuttgart 1997–2001.

[12] C. Lee, W. Yang, R. G. Parr, *Phys. Rev. B* **1988**, *37*, 785.

[13] S. Grimme, *J. Comput. Chem.* **2006**, *27*, 1787.

[14] O. Gunnarsson, B. I. Lundquist, *Phys. Rev. B* **1976**, *13*, 4274.

[15] N. Troullier, J. L. Martins, *Phys. Rev. B* **1991**, *43*, 1993.

[16] M. Boero, M. Parrinello, K. Terakura, H. Weiss, *Mol. Phys.* **2002**, *100*, 2935.

[17] S. G. Louie, S. Froyen, M. L. Cohen, *Phys. Rev. B* **1982**, *26*, 1738.

[18] M. J. Frisch, G. W. Trucks, H. B. Schlegel, G. E. Scuseria, M. A. Robb, J. R. Cheeseman, G. Scalmani, V. Barone, G. A. Petersson, H. Nakatsuji, X. Li, M. Caricato, A. V. Marenich, J. Bloino, B. G. Janesko, R. Gomperts, B. Mennucci, H. P. Hratchian, J. V. Ortiz, A. F. Izmaylov, J. L. Sonnenberg, D. Williams-Young, F. Ding, F. Lipparini, F. Egidi, J. Goings, B. Peng, A. Petrone, T. Henderson, D. Ranasinghe, V. G. Zakrzewski, J. Gao, N. Rega, G. Zheng, W. Liang, M. Hada, M. Ehara, K. Toyota, R. Fukuda, J. Hasegawa, M. Ishida, T. Nakajima, Y. Honda, O. Kitao, H. Nakai, T. Vreven, K. Throssell, J. A. Montgomery Jr., J. E. Peralta, F. Ogliaro, M. J. Bearpark, J. J. Heyd, E. N. Brothers, K. N. Kudin, V. N. Staroverov, T. A. Keith, R. Kobayashi, J. Normand, K. Raghavachari, A. P. Rendell, J. C. Burant, S. S. Iyengar, J. Tomasi, M. Cossi, J. M. Millam, M. Klene, C. Adamo, R. Cammi, J. W. Ochterski, R. L. Martin, K. Morokuma, O. Farkas, J. B. Foresman, D. J. Fox, *Gaussian16 Revision A.03*, Gaussian, Inc., Wallingford, CT **2016**.

[19] P. Atkins, J. de Paula, J. Keeler, *Atkins' Physical Chemistry*, 11th ed., Oxford University Press, Oxford **2018**, p. 560.

[20] J. R. Anglin, W. Ketterle, *Nature* **2002**, *416*, 211.

[21] W. Ketterle, *Chem. Phys. Chem.* **2002**, *3*, 736.

[22] K. B. Davis, M.-O. Mewes, M. R. Andrews, N. J. van Druten, D. S. Durfee, D. M. Kurn, W. Ketterle, *Phys. Rev. Lett.* **1995**, *75*, 3969.

[23] L. N. Cooper, *Phys. Rev.* **1956**, *104*, 1189.

[24] J. Bardeen, L. N. Cooper, J. R. Schrieffer, *Phys. Rev.* **1957**, *108*, 1175.

[25] N. Marzari, D. Vanderbilt, *Phys. Rev. B* **1997**, *56*, 12847.

[26] T. Ikeda, M. Boero, *J. Chem. Phys.* **2015**, *143*, 194510.

[27] P. L. Silvestrelli, A. Ambrosetti, *J. Chem. Phys.* **2019**, *150*, 164109.

[28] J. M. Foster, S. F. Boys, *Rev. Mod. Phys.* **1960**, *32*, 300.

[29] R. B. Woodward, R. Hoffmann, *Angew. Chem., Int. Ed.* **1969**, *8*, 781.

SUPPORTING INFORMATION

Additional supporting information may be found online in the Supporting Information section at the end of this article.